

# HIGH-RESOLUTION LOCAL IMAGING USING A MICRO-CT

*Soo Yeol Lee, Min Hyoung Cho, Jeong Min Choi*

Dept. of Biomedical Engineering, Kyung Hee University, Korea

## ABSTRACT

An x-ray micro-tomography system has been developed for *in vivo* small animal imaging studies. For efficient *in vivo* scanning, it has a rotating gantry on which the x-ray source and the flat panel x-ray detector are mounted. To reconstruct artifact-free images of a small local region inside the animal subject from the truncated projection data, the projection data from the large field of view (FOV) scan of the whole animal subject are combined with the projection data from the small FOV scan of the region of interest. For the acquisition of x-ray projection data, a  $1248 \times 1248$  flat-panel x-ray detector with the pixel pitch of  $100 \mu\text{m}$  has been used. The developed system has the spatial resolution of 12 lp/mm when the highest magnification ratio of 5:1 is applied to the zoom-in imaging.

**Index Terms**— micro-CT, zoom-in imaging, small animal imaging, rotating gantry, flat panel x-ray detector

## 1. INTRODUCTION

Micro-CT or micro-tomography is one of the widely used small animal imaging devices [1]. In many kinds of biomedical studies, it is very important to take images of animal models in a non-invasive way since longitudinal observations for a long period without sacrificing the animal models are essential. Investigating new drug effects or cell therapy effects on small animals having human disease models is one of the examples. The clear advantage of a micro-CT over other small animal imaging modalities is in its micron-resolution imaging capability. The micron-resolution imaging capability of micro-CTs has been greatly utilized in high resolution imaging of complex-structured tissues such as trabecular bones, micro vessels, and lung tissues [2-6].

In order to take whole-body images of a live animal using a micro-CT, the field of view (FOV) of the micro-CT should be bigger than the animal size. Using a large-area flat panel detector in a micro-CT, it is now possible to take whole body images of an adult rat [7,8]. However, we often have to compromise the spatial resolution of the micro-CT since high magnification is not allowed in large FOV imaging. To obtain high resolution images of a region of interest (ROI) in the animal subject, the zoom-in micro-tomography technique has been introduced [9]. Using the

zoom-in micro-tomography technique, *in vivo* rat femur imaging has been successfully performed for longitudinal observation of trabecular thickness changes in Sprague-Dawley (SD) rats raised with the osteoporosis model.

In most micro-CTs, the animal subjects are rotated for the CT scanning. However, rotating the gantry, while the animal subject lying in a natural posture, is more desirable in small animal imaging to reduce motion artifacts. Rotating-gantry-based micro-CTs are now commercially available, but, they have no high resolution ROI imaging capability. In this study, we introduce a rotating-gantry-based x-ray micro-CT system which is capable of high-resolution zoom-in imaging of a small ROI inside the animal subject.

## 2. ROTATING-GANTRY-BASED MICRO-CT

For zoom-in micro-tomography, we need to acquire two kinds of projection data sets, one from the full FOV scanning of the whole body of the animal subject and the other from the limited FOV scanning of a ROI inside the subject. The limited FOV scanning is targeted to the ROI inside the subject with a larger magnification than the full FOV scanning. Even though the limited FOV projection data has better spatial resolution than the full FOV projection data, artifact-free images cannot be reconstructed from the limited FOV projection data due to their incompleteness, i.e., truncation of the projection data outside the FOV. The artifacts cause contrast anomaly especially in the region near the boundary of ROI. In zoom-in micro-tomography, the missing projection data outside the FOV is estimated from the full FOV projection data as depicted in Fig.1. Once the missing projection data has been calculated from the full FOV projection data, the calculated projection data outside the FOV is augmented to the limited FOV projection data to reconstruct artifact-free images of the ROI [9,11].

We have made a rotating gantry on which a sliding mechanism is mounted as shown in Fig. 2 [11]. The rotating gantry is made of a circular aluminum plate with the diameter and thickness of 540mm and 20mm, respectively. The sliding mechanism, depicted as the linear motion (LM) actuator with the aluminum mount on it and the size of  $85 \times 65 \times 570 \text{ mm}^3$ , is mounted on the rotating gantry. The LM actuator is driven by a servo motor through a ball screw

with the pitch of 3 mm. The angular resolution of the servo motor is  $0.036^\circ$  which makes the sliding precision be  $\pm 0.3 \mu\text{m}$ . The rotating gantry is driven by another servo motor with the angular resolution of  $0.036^\circ$ . The servo motor is coupled with the rotating gantry through a 100:1 speed reduction gear. With the speed reduction gear, the rotational motion of the rotating gantry can be controlled with the angular resolution of  $3.6 \times 10^{-4}^\circ$ . The rotation speed can be controlled from 1.5 min to 30 min per rotation. Since one rotation suffices for a 3-dimensional imaging with a flat-panel detector, flexible cables are used for all the electrical wirings between the system controller and the rotating gantry without using slip rings. The x-ray source and the x-ray detector are fixed on the aluminum mount which is movable along the ball screw in the sliding mechanism. The relative positions of the x-ray source and the x-ray detector with respect to the rotational center are controlled by sliding mechanism. The x-ray source to detector distance,  $SD$ , has been set to 456 mm, and the x-ray source to the animal subject distance,  $SO$ , has been controlled between 91 mm and 380 mm, which makes the magnification ratio vary from 1.2:1 to 5.0:1.

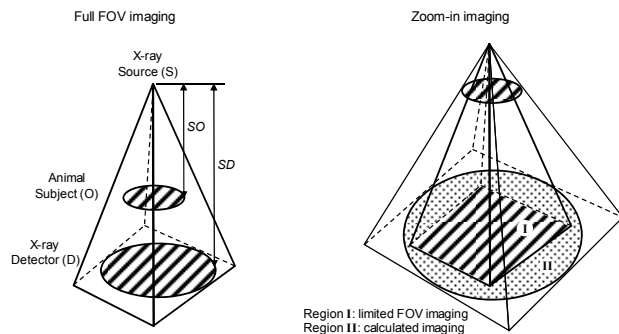


Fig. 1 Full FOV imaging and zoom-in imaging. In zoom-in imaging, the projection data outside the detector area (region II) are calculated from the full FOV projection data.

We used a micro-focus x-ray source (5000Apogee, Oxford Instruments, USA) which has a rather large nominal focal spot size of  $35 \mu\text{m}$ . The x-ray tube is a sealed tube with a fixed tungsten anode having an angle of  $11^\circ$  against the electron beam and with a  $127 \mu\text{m}$ -thick beryllium exit window. The emitted x-ray beam angle is about  $22^\circ$ . The maximum tube voltage and tube current are 50 kV and 1 mA, respectively. The micro-focus x-ray source has been operated in a continuous mode with an Al filter with the thickness of 1mm. We used a commercially available flat-panel detector (C7943SPL, Hamamatsu, Japan) to acquire 2D x-ray projection data. The flat-panel detector consists of a  $1248 \times 1248$  active matrix of transistors and photodiodes

with a pixel pitch of  $100 \mu\text{m}$ , and a CsI:Tl scintillator. The sensitive area of the detector is about  $12 \times 12 \text{ cm}^2$  which is large enough to cover an adult SD rat.

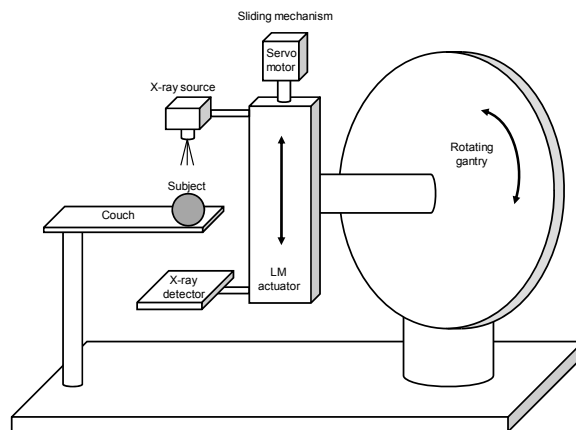


Fig. 2 The schematic diagram of the rotating-gantry based micro-CT

### 3. IMAGING STUDIES

In the image reconstruction, 3D whole body images are firstly reconstructed from the full FOV projection data set using the Feldkamp algorithm [10]. Before applying the 3D reconstruction algorithm, we applied flat field correction and dead pixel/line correction to the acquired 2D projection data to avoid ring artifacts in the reconstructed images. After reconstructing the full FOV 3D images, we calculated the missing projection data outside the FOV in the limited FOV scan as shown in Fig. 1. The missing projection data in the region II has been calculated by ray-tracing the full FOV 3D images. We scaled the calculated projection data so that the two projection data sets, one acquired by the flat-panel detector in region I and the other calculated in region II, are continuous at the interface between the two regions. After augmenting the calculated projection data to the acquired projection data, we reconstructed 3D images of the ROI using the Feldkamp algorithm.

In the previous studies, we have evaluated the spatial resolution performance of the developed micro-CT [11]. To secure high resolution in the zoom-in imaging, it is essential to match the full FOV data exactly with the limited FOV data before the image reconstruction. Since we take the images twice changing the magnification ratio, there might be mismatches between the two data caused by the translation and tilt of the subject during the linear motion on the sliding mechanism. We have found the translational shift and tilt angle using the calibration plate as mentioned in the previous studies [9]. After reconstructing 3D images

from the full FOV data, we apply the translation and tilt to the 3D image in the reverse direction for the correction. We have found that the mismatches between the two projection data may degrade spatial resolution particularly in the boundary region of the ROI.

For the spatial resolution measurements, we took cross-sectional images of a thin gold wire which has the diameter of 20  $\mu\text{m}$ . From the gold wire image, we have calculated the MTF of the micro-CT taking into account the non-zero width of the gold wire. From the MTF measurements, the spatial resolutions of the micro-CT have been estimated to be about 12 lp/mm and 4 lp/mm in the zoom-in imaging and the full FOV imaging, respectively.

*In vivo* small animal imaging has been performed with an adult SD rat weighing 400 g. The *in vivo* animal imaging has been performed at 40 kVp and 0.55 mA. During the scan, the rat was anesthetized with combination of 1.5% isoflurane (Choong-Wae Pharma Co., Korea), 70% N<sub>2</sub>O and 30% O<sub>2</sub> gas, and the anesthetizing gas was delivered with a gas anesthesia machine (Tabletop research anesthesia machine sets, SurgiVet, USA).

#### 4. EXPERIMENTAL RESULTS

The cross-sectional images of a live adult SD rat are shown in Fig. 3. Figure 3(a) shows the full FOV image at the femur bone region. The femur bone region (the circled area) was chosen to be the ROI. Figure (b) shows the digitally magnified image in the femur bone region. Due to the limited spatial resolution, the trabecular bone structure is not clearly seen in the magnified image. Figure 3(c) shows the ROI image obtained with the zoom-in micro-tomography technique. Owing to its better spatial resolution, the visibility of the trabecular bone structure is now much improved in Fig. 3(c).

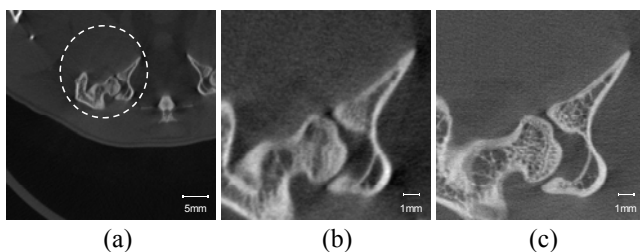


Fig. 3 (a) The full FOV imaging of a rat, (b) the digitally magnified image of the circled region in (a), and (c) the femur image obtained with the zoom-in imaging technique

#### 5. DISCUSSION AND CONCLUSION

The rotating-gantry-based micro-CT has many advantages over a conventional micro-CT in which the animal subject is rotated during the tomographic scan. By rotating the x-ray

source and x-ray detector pair for the scan while the animal subject lying in a natural posture, we can be freed from many problems related with rotating the animal subject. With the rotating-gantry-based micro-CT, we expect less motion artifacts in the reconstructed images, bigger survival rate of the animal subjects during the studies with anesthetization and shorter preparation time for the scan. The animal subject lying in a natural posture also allows physiological monitoring like ECG more easily.

Unlike the commercial rotating-gantry-based micro-CT system, the developed micro-CT system has the sliding mechanism on the rotating gantry for the zoom-in imaging. Bony tissue imaging for osteoporosis studies and micro vessel imaging for angiogenesis studies seem to be promising application areas. Recently, trabecular thickness measurement has been tried on live rats with the zoom-in micro-tomography technique [6]. With rat models having ovariectomy-induced osteoporosis, they successfully observed thinning process of the trabecular bones over several weeks without sacrificing them. We used the x-ray tube having rather large focal spot size to secure proper x-ray exposure level. To obtain better spatial resolution on the order of micron, an x-ray tube having smaller focal spot size may be used. But, it should be verified that the mechanical precision of the rotating gantry is good enough not to lose the benefit of the smaller focal spot size.

Motion artifacts are still great nuisances in small animal imaging with micro-CTs. Unlike human scans with clinical x-ray CTs, micro-CT images have poor SNR due to the much smaller pixel size and much lower exposure level than clinical scans. It seems that soft tissue visibility in small animal studies with a micro-CT cannot be ensured with a scan time shorter than a respiration period of small animals whatever detector types are used. Motion artifacts in zoom-in micro-tomography should be investigated in the future imaging studies of live small animals.

In conclusion, a rotating-gantry-based zoom-in micro-CT has been successfully used for *in vivo* imaging studies of the trabecular bone structure in rats having osteoporosis models. We expect that the proposed system can be greatly used for many other *in vivo* small animal imaging applications.

#### ACKNOWLEDGEMENTS

This study was supported by a grant of the Korea Health 21 R&D Project, Ministry of Health and Welfare (02-PJ3-PG6-EV07-0002) and a grant from the Korea Science and Engineering Foundation (R11-2002-103).

#### REFERENCES

- [1] R. Weissleder, and U. Mahmood, "Molecular imaging,"

*Radiology*, vol. 219, pp. 316-333, 2001.

- [2] M.J. Paulus, H. Sari-Sarraf, S.S. Gleason, M. Bobrek, J.S. Hicks, D.K. Johnson, J.K. Behel, L.H. Thompson, and W.C. Allen, "A new x-ray computed tomography system for laboratory mouse imaging," *IEEE. Trans. Nucl. Sci.*, vol. 46, pp. 558-564, 1999.
- [3] S.Y. Wan, A.P. Kiraly, E.L. Ritman, and W.E. Higgins, "Extraction of the hepatic vasculature in rats using 3-D micro-CT images," *IEEE. Trans. Med. Imag.*, vol. 19, pp. 964-971, 2000.
- [4] E.L. Ritman, "Molecular imaging in small animals-roles for micro-CT," *J. Cell. Biochem. Supp.*, vol. 39, pp. 116-124, 2002.
- [5] R.D. Kapadia, G.B. Stroup, A.M. Badger, B. Koller, J.M. Levin, R.W. Coatney, R.A. Dodds, X. Liang, M.W. Lark, and M. Gowen, "Application of micro-CT and MR microscopy to study pre-clinical models of osteoporosis and osteoarthritis," *Technol. Health Care*, vol. 6, pp. 361-372, 1998.
- [6] I.K. Chun, M.H. Cho, J.H. Park, and S.Y. Lee, "In vivo trabecular thickness measurement in cancellous bones: longitudinal rat imaging studies," *Physio. Meas.*, vol. 27, pp. 695-702, 2006.
- [7] D.A. Jaffray, and J.H. Siewerdsen, "Cone-beam computed tomography with a flat-panel imager: initial performance characterization," *Med. Phys.*, vol. 27, pp. 1311-1123, 2000.
- [8] S.C. Lee, H.K. Kim, I.K. Chun, M.H. Cho, S.Y. Lee, and M.H. Cho, "A flat-panel detector based micro-CT system: performance evaluation for small-animal imaging," *Phys. Med. Biol.*, vol. 48, pp. 4173-4185, 2003.
- [9] I.K. Chun, M.H. Cho, S.C. Lee, M.H. Cho, and S.Y. Lee, "X-ray micro-tomography system for small-animal imaging with zoom-in imaging capability," *Phys. Med. Biol.*, vol. 49, pp. 3889-3902, 2004.
- [10] L.A. Feldkamp, L.C. Davis, and J.W. Kress, "Practical cone-beam algorithm," *J. Opt Soc. Am. A*, vol. 1, pp. 612-619, 1984.
- [11] M.H. Cho, D.H. Lee, B.H. Han, S.Y. Lee, "Rotating-gantry-based x-ray micro-tomography system with the sliding mechanism capable of zoom-in imaging," *J. Biomed. Eng. Res.* in press, 2008.